Journal of Hydrology 364 (2009) 152–162

Contents lists available at ScienceDirect

Journal of Hydrology

journal homepage: www.elsevier.com/locate/jhydrol

Low frequency drought variability associated with climate indices

Mehmet Özger *, Ashok K. Mishra, Vijay P. Singh

Dept. of Biological and Agricultural Engineering, Texas A&M Univ., College Station, TX 77843-2117, USA

ARTICLE INFO

Article history:
Received 19 July 2008
Received in revised form 14 October 2008
Accepted 21 October 2008

Keywords:
ENSO
Spatial variation
Drought
Wavelet transforms
Kriging

SUMMARY

The variability in the sea surface temperature (SST) in the Pacific Ocean has an influence on the variability of the continental US precipitation, streamflow and drought. Analysis of the dominant oscillations of droughts and large-scale climate indices shows that interannual and interdecadal variations related to climate indices are significant indicators of drought occurrences. Using wavelet transforms and cross-correlations and Kriging, spatial structure of teleconnections of both El Niño Southern oscillation (ENSO) and Pacific decadal oscillation (PDO) to droughts during the 20th century is investigated, with particular reference to the state of Texas. Each region in Texas has different responses but arid regions show stronger correlations to climate anomalies than do sub-tropic humid regions. Lag times and correlation coefficients between droughts and climate indices are detected. Maps indicating the spatial variations of lag times and correlation coefficients are presented for annual and decadal scales. The proposed investigation permits to determine lag times between drought characteristics and climate indices along with significant correlations; these features are different from those of existing methods. Decision makers in the field of water resources management and agriculture can benefit from the evaluation of the ENSO variability and drought variability.

Introduction

The association of North American hydrologic droughts and El Niño Southern oscillation (ENSO) has received significant attention in recent years (Piechota and Dracup, 1996; Trenberth and Branstator, 1992; Cole and Cook, 1998). Halpert and Ropelewski (1992) and Kiladis and Diaz (1989) reported a strong relationship between ENSO and seasonal mean anomalies of precipitation and temperature which are considered key factors for the initiation of a drought. McCabe and Dettinger (1998), Dettinger et al. (1995, 1998), and Cayan et al. (1998) investigated temporal variations in the ENSO teleconnections to the US climate and they found a decadal variability in the ENSO teleconnections to western US precipitation. Cole and Cook (1998) noted changes in the spatiotemporal variability in US summer Palmer drought severity index (PDSI).

Rajagopalan and Cook (2000) investigated the spatial structure of teleconnections between both the winter ENSO and global sea surface temperatures (SSTs), and a measure of continental US summer drought during the 20th century. They concluded that during the first three decades of this century, summer drought teleconnections in response to SST patterns linked to ENSO were the strongest in the southern region of Texas, with extensions into regions of the Midwest. Barlow et al. (2001) found a significant relationship between three primary modes of Pacific variability [ENSO, Pacific decadal oscillation (PDO), and the North Pacific mode (NPM)] and the US warm season precipitation, drought, and stream flow. They found that the relationships with drought and stream flow varied little throughout the season, but the relationship with precipitation varied substantially from month to month. Barros and Bowden (2008) proposed an approach to extend the lead time of operational drought forecasts up to 12 months by considering ENSO.

Climate anomalies can cause different effects in different regions. Zhang et al. (2007) showed that different phase relations existed in the lower, the middle and the upper Yangtze River basin in China. In-phase relations were detected between annual maximum streamflow of the lower Yangtze River and anti-phase relations were found in the upper Yangtze River. But ambiguous phase relations occured in the middle Yangtze River, showing that the middle Yangtze River basin was a transition zone. Different climate systems controlled the upper and the lower Yangtze River. Tootle et al. (2008) evaluated the Pacific and Atlantic Ocean SSTs and Colombian streamflow to identify coupled regions of SST and Colombian streamflow variability. They revealed that the warmer (cooler) equatorial SSTs resulted in lesser (greater) streamflow. Pongracz et al. (1999) applied fuzzy rule-based modeling to the prediction of regional droughts using two forcing inputs, ENSO and large-scale atmospheric circulation patterns. Chiew et al. (1998) presented an overview of the relationship between ENSO

* Corresponding author. Tel.: +1 9797392751.
E-mail addresses: mehmetozger@tamu.edu (M. Özger), amishra@tamu.edu (A.K. Mishra), vsingh@tamu.edu (V.P. Singh).

0022-1694/$ - see front matter © 2008 Elsevier B.V. All rights reserved.
doi:10.1016/j.jhydrol.2008.10.018

and rainfall, drought and streamflow in Australia. They showed that dry conditions in Australia tend to be associated with El Niño.

Droughts can show a variable pattern at spatial scales depending on their severity and duration. A consistent response to large-scale climate patterns can appear in regional drought occurrences. Recently, there has been considerable interest in the use of climate indices for long-term forecasts of regional droughts. But there are still questions as to how SST states affect the spatial structure of droughts. The variation in the relationship between SST anomalies and drought indices at annual to decadal timescales is of particular interest.

In this paper, variability and possible teleconnections between drought occurrences and large-scale climate indices, such as ENSO which is here represented by sea surface temperature anomalies for different regions (NINO 3, NINO 3.4, etc.) in the Pacific Ocean, and PDO were investigated using continuous wavelet transform (CWT), cross-correlation and Kriging, and cross wavelet approaches. The drought occurrences were quantified by the palmer drought severity index (PDSI). The specific objectives of the study therefore are: (1) to identify the dominant oscillations of drought indices and their temporal variations using CWT; (2) to determine the spatial correlation structure between large-scale climate and drought indices with the aim at detecting the response of regions with respect to various large-scale climate anomalies, such as ENSO and PDO; (3) to relate the drought variability to large-scale anomalies at annual and decadal scales; and (4) to determine the phase relations between PDSI and climate anomalies for all climate divisions in Texas.

Methodology

Spatial structure of teleconnections of both ENSO and PDO to droughts along with the scale analysis was investigated using wavelet transforms, correlations and spatial analysis. For this purpose CWT, cross-correlation and Kriging approaches were used, and a flow chart of methodology is shown in Fig. 1.

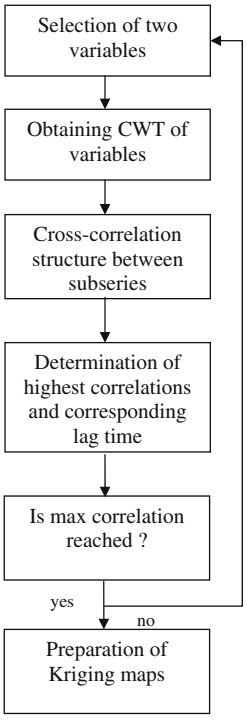

Figure 1. Flow chart of proposed approach.

Continuous wavelet transform

The continuous wavelet transform (CWT) is used to decompose a signal into wavelets, small waves that grow and decay over a small distance, whereas the Fourier transform decomposes a signal into infinite number of terms of sines and cosines losing most time-localization information. A continuous wavelet transform of a signal produces the coefficients at a given scale. Comparison between Fourier analysis and wavelet analysis is given by Kumar and Foufoula-Georgiou (1997) who presented only the basics regarding wavelet analysis. The CWT's basis functions are scaled and shifted versions of the time-localized mother wavelet. A Morlet wavelet is one of the many wavelet functions which has a zero mean and is localized in both frequency and time. Since the Morlet wavelet provides a good balance between time and frequency localizations, it is preferred for application. It can be represented as [Torrence and Compo, 1998; Torrence and Webster, 1999; Grinsted et al., 2004]

$$\psi(\eta) = \pi^{-1/4} e^{i\omega\eta - 0.5\eta^2} \tag{1}$$

where ω is the dimensionless frequency, and η is the dimensionless time parameter. The wavelet is stretched in time (t) by varying its scale (s), so that $\eta = s/t$. When using wavelets for feature extraction purposes, the Morlet wavelet (with $\omega = 6$) is a good choice, since it satisfies the admissibility condition (Farge, 1992; Torrence and Compo, 1998).

For a given wavelet $\psi_0(\eta)$, it was assumed that X_j is a time series of length N (X_j, $i = 1,\ldots,N$) with equal time spacing δt. The continuous wavelet transform of a discrete sequence X_j is defined as convolution of X_j with the scaled and translated wavelet, $\psi_0(\eta)$:

$$W_n^X(s) = \sum_{j=1}^{N} X_j \psi^* \left[\frac{(j-n)\delta t}{s}\right] \tag{2}$$

where the asterisk indicates the complex conjugate. CWT decomposes time series into time–frequency space, enabling the identification of both the dominant modes of variability and how those modes vary with time.

Cross wavelet transform

Torrence and Compo (1998) defined the cross wavelet spectrum of two time series X and Y with wavelet transform W_n^X and W_n^Y as

$$\left|W_n^{XY}(s)\right| = \left|W_n^X(s) \cdot W_n^{*Y}(s)\right| \tag{3}$$

where W_n^{*Y} is the complex conjugate of W_n^Y. The complex argument of W_n^{XY} can be interpreted as the local relative phase between time series X_j and Y_j. Statistical significance is estimated against a red noise model (Torrence and Compo, 1998). Thus cross wavelet transform (XWT) can be constructed from two CWTs. XWT denotes their common power and relative phase in time-frequency space.

Correlation analysis

Once the CWT coefficients of each variable are obtained, it is possible to evaluate all scales between two different variables. Cross-correlation was used to show the relationship between two variables at different scales. Cross-correlation structure reveals that the effective scales which exhibit a strong relationship between two variables and also the corresponding lag time where the correlation coefficient reaches its maximum value. A sample cross-correlation function of NINO 3.4 and PDSI for different scales is shown in Fig. 2. It is seen from this figure that the highest correlation coefficients of 0.7 and 0.8 with lag times greater than 10 months were obtained for the 8 and 16 year scales, respectively.